

Parametrically Excited Surface Waves: Two-Frequency Forcing, Normal Form Symmetries, and Pattern Selection

Mary Silber

*Department of Engineering Sciences & Applied Mathematics
Northwestern University
Evanston, IL 60208, USA*

Anne C. Skeldon

*Department of Mathematics
City University, Northampton Square
London, EC1V 0HB, UK*

October 1, 1998

Abstract

Motivated by experimental observations of exotic free surface standing wave patterns in the two-frequency Faraday experiment, we investigate the role of normal form symmetries in the associated pattern selection problem. With forcing frequency components in ratio m/n , where m and n are co-prime integers that are not both odd, there is the possibility that both harmonic waves and subharmonic waves may lose stability simultaneously, each with a different wavenumber. We focus on this situation and compare the case where the harmonic waves have a longer wavelength than the subharmonic waves with the case where the harmonic waves have a shorter wavelength. We show that in the former case a normal form transformation can be used to remove all quadratic terms from the amplitude equations governing the relevant resonant triad interactions. Thus the role of resonant triads in the pattern selection problem is greatly diminished in this situation. We verify our general bifurcation theoretic results within the example of one-dimensional surface wave solutions of the Zhang-Viñals model [1] of the two-frequency Faraday problem. In one-dimension, a $1 : 2$ spatial resonance takes the place of a resonant triad in our investigation. We find that when the bifurcating modes are in this spatial resonance, it dramatically effects the bifurcation to subharmonic waves in the case that the forcing frequencies are in ratio $1/2$; this is consistent with the results in [1]. In sharp contrast, we find that when the forcing frequencies are in ratio $2/3$, the bifurcation to (sub)harmonic waves is insensitive to the presence of another spatially-resonant bifurcating mode. This is consistent with the results of our general analysis.

PACS numbers: 47.54.+r, 47.20.Ky, 47.35.+i

1 Introduction.

Exotic free surface standing wave patterns, parametrically excited by two-frequency forcing, have attracted considerable attention in recent years, both experimentally [2, 3, 4, 5] and theoretically [1, 6, 7, 8, 9]. In this system, the surface waves are excited by subjecting the fluid layer to a time-periodic vertical acceleration with two (rationally-related) frequency components. This corresponds to a modification of a classic hydrodynamic problem, which dates back to observations of Faraday [10], in which the surface waves are parametrically excited by a purely sinusoidal vertical acceleration of the fluid container [11]. Triangular patterns [4], quasi-patterns [3, 5], and superlattice patterns [5] are among the more exotic states that have been observed in laboratory experiments employing two-frequency forcing. Here, “quasi-patterns” are patterns with twelve-fold symmetry and are the hydrodynamic analogues of two-dimensional quasi-crystals. These patterns are not spatially-periodic, but do have long-range orientational order; their spatial Fourier transform exhibits twelve prominent equally-spaced peaks that lie on a circle. Although such patterns have been observed in single-frequency Faraday experiments [12, 13, 14], they are more readily observed with two-frequency forcing and examples have been seen with excitation frequencies in ratio 4/5, 4/7, 6/7, 8/9 [3]. In contrast, “superlattice” patterns are spatially-periodic with structure on two disparate length-scales. They have been observed in the two-frequency Faraday system with a forcing frequency ratio of 6/7 [5]. The observations of both quasipatterns and superlattice patterns have indicated that the patterns are *synchronous* with the forcing frequency. The Faraday wave problem is an attractive experimental system for studying the fundamental mechanisms behind the occurrence of such patterns because of the fast time scales involved and the number of tunable control parameters [15, 16].

One motivation behind some of the early experiments on two-frequency parametric excitation of Faraday waves was to destroy the Z_2 symmetry associated with subharmonic waves [2, 3, 4]. Specifically, in the classic Faraday experiment with single-frequency forcing $\cos(\omega t)$, the onset surface waves respond subharmonically with frequency $\omega/2$ [17]. (Harmonic response is also possible for very shallow layers of viscous fluid [18, 19].) In the situation of subharmonic response there is a discrete time translation symmetry $t \rightarrow t + \frac{2\pi}{\omega}$ that is broken by the state of the system. This symmetry-breaking manifests itself in the governing pattern amplitude equations by suppressing all even terms. Whether or not this extra Z_2 symmetry is present has a particularly profound effect on the formation of hexagonal patterns [20]; for instance, in many systems where it is absent, hexagonal patterns are preferred at onset [21]. Edwards and Fauve [3] noted that by introducing the second perturbing frequency component to the periodic forcing, they could destroy the discrete time translation symmetry of the system.

A second feature of using two frequency forcing is that it is possible to obtain a neutral stability curve with minima at two distinct wavenumbers, where the ratio of these two critical wavenumbers can be adjusted by varying the two frequency components of the forcing. Typically, one minimum corresponds to standing waves that are subharmonic with respect to the forcing frequency, while the other minimum corresponds to synchronous waves [7]. It was proposed by Edwards and Fauve [3] that by tuning the ratio of wavenumbers of the most unstable modes one could control the resonant triad interactions that are important to the pattern formation process [22]. Indeed all of the exotic patterns mentioned above were obtained with experimental parameters near the so-called “bicritical point” where two modes lose stability

simultaneously [3, 4, 5].

The role of resonant triad interactions in the formation of Faraday wave patterns has been investigated extensively by Viñals and co-workers for both the case of single frequency forcing [23, 24], and two-frequency forcing [1]. The most detailed two-frequency calculations focused on the situation where the frequency ratio was $1/2$, and the onset surface wave response was subharmonic with the forcing. Zhang and Viñals compared their theoretical results with experimental results of Müller [4], who observed subharmonic hexagons, triangles and squares near the bicritical point; which pattern was observed depended on a relative phase between the ω and 2ω sinusoidal waveforms in the forcing function. A key theoretical idea behind the work of Zhang and Viñals [1, 24], and Chen and Viñals [23] is that the presence of certain resonant triads composed of Fourier mode wavevectors \mathbf{k}_1 , \mathbf{k}_2 and $\mathbf{k}_1 + \mathbf{k}_2$ ($|\mathbf{k}_1| = |\mathbf{k}_2|$) can suppress the formation of regular wave patterns that involve the \mathbf{k}_1 and \mathbf{k}_2 modes. In particular, this is the case when the \mathbf{k}_1 and \mathbf{k}_2 modes are excited at the onset of the Faraday wave instability, while the mode with wave vector $\mathbf{k}_1 + \mathbf{k}_2$ is only weakly damped. This situation arises quite naturally near the bicritical point in parameter space.

Motivated by the ubiquity of quasi-patterns in two-frequency Faraday experiments, Lifshitz and Petrich [8] recently investigated twelve-fold quasi-patterns within the framework of a simple Swift-Hohenberg type model for the evolution of a real scalar field $u(\mathbf{x}, t)$. Their model lacks reflection-symmetry $u \rightarrow -u$, and the linearized equations lead to a neutral stability curve with a double absolute minimum. However, because their model leads to time-independent patterns arising from steady state bifurcation, it does not capture one of the key features of the two-frequency Faraday problem. Specifically, at the bicritical point in the Faraday problem, one of the neutral curve minima is associated with a Floquet multiplier (FM) $+1$, while the other minimum is associated with a FM of -1 . In this paper we are specifically interested in this feature of the bicritical point of the two-frequency Faraday experiment, and its potential influence on the resonant triad interactions important to the pattern formation problem.

We investigate the role of resonant triads in the formation of wave patterns near the bicritical point in parameter space. We focus on the situation that applies to the two-frequency quasipattern [3] and superlattice pattern [5] experiments in which the forcing frequency ratio, $m/n < 1$, has m even and n odd. We show that the usual contribution of resonant triads to the cross-coupling coefficient in the amplitude equations may be greatly *suppressed* in this case. This is in marked contrast to the situation of subharmonic waves with forcing ratio $m/n < 1$, where m is odd and n is even, *e.g.* $m/n = 1/2$, as studied by Zhang and Viñals. In this latter case, resonant triads lead to peaks in the cross-coupling coefficient $g(\theta)$ [1]. In order to understand the distinction between these two situations, we first recall that in each of these cases the neutral stability curve has a double absolute minimum at the bicritical point, with one of the minima associated with a FM = $+1$ and the other with a FM = -1 [3, 7]. At the bicritical point, there are two distinct critical wavenumbers, k_m and k_n ($k_m < k_n$). The FM = $+1$ is associated with the smaller critical wavenumber k_m if the even frequency is less than the odd one (*i.e.*, $m/n = \text{even/odd}$); and it is associated with the larger wavenumber k_n if the even frequency is *greater* than the odd one (*i.e.*, $m/n = \text{odd/even}$). We show that in the former case the normal form of the coupled amplitude equations describing the relevant resonant triad interaction does not possess any quadratic terms because of a symmetry associated with the subharmonic waves. This is in contrast to the case of odd/even forcing where quadratic terms are present in the normal form.

In this paper, we demonstrate this distinction between even/odd and odd/even forcing by considering a simple example of one-dimensional waves that are parametrically excited by two frequencies. Rather than consider the full hydrodynamic equations, we investigate this issue using a simpler model derived from the free-surface Navier-Stokes equation by Zhang and Viñals [24]; their model applies to a deep layer of low-viscosity fluid. We consider both $2\omega/3\omega$ and $1\omega/2\omega$ forcing frequencies, over a range of frequencies ω , including a critical frequency for which a one-dimensional spatial resonance occurs. Specifically, at the critical frequency, the minima at the bicritical point are in ratio $k_m/k_n = 1/2$. We find that this spatial resonance leads to a divergence of the Landau coefficient in the amplitude equation describing bifurcation to subharmonic waves in the case of the $1/2$ forcing frequency ratio; this is consistent with the results of Zhang and Viñals [24]. In contrast, the Landau coefficient for waves, parametrically excited by two-frequency forcing in ratio $2/3$, is unaffected by any parameter proximity to the bicritical point and/or the spatial resonance point. While the wave vectors of the critical modes \mathbf{k}_1 and $2\mathbf{k}_1$ are in resonance, there is a mismatch in their frequencies: in this case the usual large contribution to the Landau coefficient due to the spatial resonance is absent.

The next section of the paper provides the necessary background to our analysis. It reviews the key theoretical ideas about the role of resonant triad interactions in pattern formation problems, as well as the linear theory for Faraday waves, parametrically excited by two-frequency forcing. This background section closes with a discussion of the normal form symmetries associated with the subharmonic instability. Section 3 sets up the example of one-dimensional surface waves, indicating the precise analogy between triad resonance in two dimensions and spatial resonance within this simpler one-dimensional problem. This section also presents the governing hydrodynamic equations that describe parametrically excited surface waves in the limit of an infinite depth fluid layer and weak viscosity. The last part of Section 3 sets up the weakly nonlinear analysis that we use to compute the cubic Landau coefficient for harmonic and subharmonic waves. Section 4 presents bifurcation results for two examples: waves parametrically excited by two-frequency excitation in the ratio $2/3$ and waves excited with a $1/2$ excitation frequency ratio. Section 5 summarizes our results, and indicates some directions for future work.

2 Background.

2.1 Resonant triad interactions.

One of the central ideas in pattern formation studies of quasi-patterns [3, 8, 14, 22], and surface wave patterns parametrically excited by two-frequency forcing [1, 3] is that of resonant triad interactions. In particular, there is interest in systems, such as the Faraday system with two-frequency forcing, for which it is possible to have a neutral stability curve with a double minimum. The resonant triad interaction of interest is dictated by the locations of the minima, say k_m and k_n , of the neutral curve. The resonant triad is made up of wave vectors \mathbf{k}_1 , \mathbf{k}_2 and $\mathbf{k}_1 + \mathbf{k}_2$, where $|\mathbf{k}_1| = |\mathbf{k}_2| = k_m$ and $|\mathbf{k}_1 + \mathbf{k}_2| = k_n$. Thus the angle θ between \mathbf{k}_1 and \mathbf{k}_2 satisfies

$$\cos\left(\frac{\theta}{2}\right) = \frac{k_n}{2k_m} . \quad (1)$$

Here we have assumed that $0 < k_m < k_n < 2k_m$; see Figure 1.

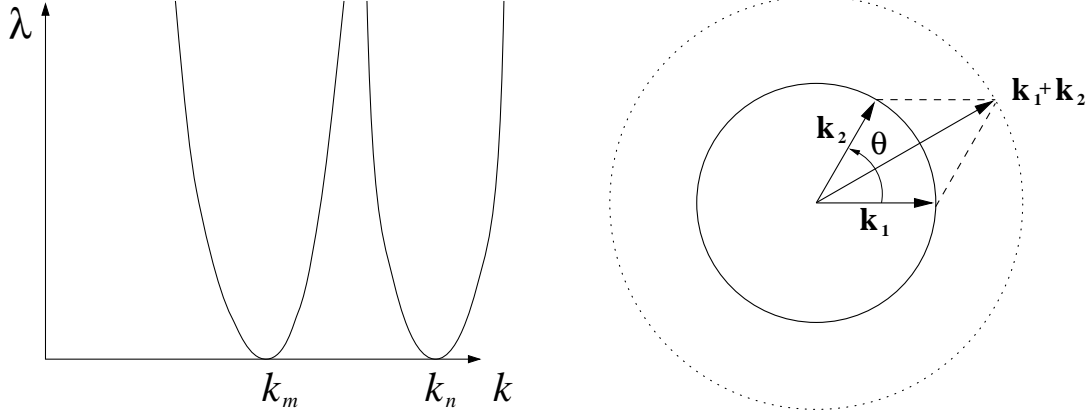


Figure 1: On the left is a plot of a neutral stability curve $\lambda(k)$, showing minima at $k = k_m$ and $k = k_n$. On the right is an associated resonant triad \mathbf{k}_1 , \mathbf{k}_2 and $\mathbf{k}_1 + \mathbf{k}_2$, where $|\mathbf{k}_1| = |\mathbf{k}_2| = k_m$ and $|\mathbf{k}_1 + \mathbf{k}_2| = k_n$. The angle θ between \mathbf{k}_1 and \mathbf{k}_2 is related to the ratio k_n/k_m by (1).

To illustrate the possible influence of resonant triad interactions on pattern formation, we first consider a steady state bifurcation problem, where modes of wavenumber k_m and k_n lose stability (almost) simultaneously with the increase of an external control parameter. We consider a bifurcation problem on a six-dimensional center manifold for linear modes

$$A(t)e^{i\mathbf{k}_1 \cdot \mathbf{x}} + B(t)e^{i\mathbf{k}_2 \cdot \mathbf{x}} + C(t)e^{i(\mathbf{k}_1 + \mathbf{k}_2) \cdot \mathbf{x}} + c.c., \quad (2)$$

where $A, B, C \in \mathbf{C}$. Symmetry considerations determine that the unfolding of the bifurcation problem takes the form, through cubic order in the amplitudes,

$$\begin{aligned} \dot{A} &= \lambda A + \alpha B^* C + (a|A|^2 + b|B|^2 + c|C|^2)A \\ \dot{B} &= \lambda B + \alpha A^* C + (a|B|^2 + b|A|^2 + c|C|^2)B \\ \dot{C} &= \mu C + \beta AB + (d|A|^2 + d|B|^2 + e|C|^2)C, \end{aligned} \quad (3)$$

where the asterisk indicates the complex conjugate, and the coefficients are all real. If $\lambda = 0$, $\mu \neq 0$, then one can further reduce the bifurcation problem to one involving the critical modes A and B , with C constrained to the center manifold: $C = -\frac{\beta}{\mu}AB + \dots$. One obtains, for $|\lambda|$ sufficiently small, the reduced (unfolded) bifurcation problem

$$\begin{aligned} \dot{A} &= \lambda A + a|A|^2 A + \left(b - \frac{\alpha\beta}{\mu}\right)|B|^2 A \\ \dot{B} &= \lambda B + a|B|^2 B + \left(b - \frac{\alpha\beta}{\mu}\right)|A|^2 B. \end{aligned} \quad (4)$$

The presence of the near critical mode C in (2) leads to a large cross-coupling coefficient $g(\theta) \equiv (b - \frac{\alpha\beta}{\mu})$ in the amplitude equations (4) since $|\mu| \ll 1$. A consequence of this is that patterns that involve an equal amplitude superposition of modes A and B tend to be unstable

at onset. For example, the stability of steady rhombic patterns at angle θ ($A = B$ in (4)), within the setting of the amplitude equations (4), is determined by two eigenvalues whose signs are $\text{sgn}(a + b - \frac{\alpha\beta}{\mu})$ and $\text{sgn}(a - b + \frac{\alpha\beta}{\mu})$. When $|\frac{\alpha\beta}{\mu}| \gg |a| + |b|$, the two eigenvalues take on opposite signs and the pattern is necessarily unstable at onset. If the spatial resonance occurs near $\theta = \pi/2$, for example, then square planforms are unstable. Quasi-patterns, and spatially-periodic “superlattice” patterns, such as described in [5, 9, 25], involving both of the modes A and B above are similarly destabilized by a large cubic cross-coupling coefficient $g(\theta)$ in the amplitude equations. This point is discussed for various regular patterns, including quasi-patterns, in [1].

2.2 Bicritical curves for the two-frequency Faraday problem.

We now examine, in greater detail, the double minimum of the neutral curve associated with the Faraday problem with two-frequency forcing. Besson, Edwards and Tuckerman [7] computed the linear stability of the flat free surface of a shallow fluid layer subjected to a periodic vertical acceleration

$$g(t) = g_0 + g_z[\cos(\chi)\cos(m\omega t) + \sin(\chi)\cos(n\omega t + \phi)]. \quad (5)$$

Here g_0 is the usual gravitational acceleration, m and n are co-prime integers, and g_z, ω, χ, ϕ are additional external control parameters. Note that the angle χ controls the relative amplitudes of the $m\omega$ -forcing and $n\omega$ -forcing. Besson *et al.* [7] compared, with good agreement, their theoretical predictions with their experimental results for various fluids with different viscosities in the case that $m = 4$ and $n = 5$ in (5). In this case, they found that the initial instability of the fluid surface was either associated with a Floquet multiplier (FM) -1 or $+1$, depending on whether the odd or even frequency component in (5) dominated. The transition between subharmonic (FM = -1) and harmonic response (FM = $+1$) occurred at a particular value of the angle χ in (5), called the bicritical point.

Here we do not consider the full hydrodynamic problem, but rather a simplified model derived by Zhang and Viñals [24], which applies to a deep layer of weakly viscous fluid. The linearized equation for the free surface mode $h_k(t)e^{ikx}$ is

$$h_k'' + 4\nu k^2 h_k' + \left[g(t)k + \frac{\Gamma k^3}{\rho} + 4\nu^2 k^4 \right] h_k = 0, \quad (6)$$

where ν is the kinematic viscosity of the fluid, Γ is the surface tension, and ρ is the fluid density. Note that in the absence of the time periodic parametric forcing (*i.e.* $g_z = 0$), one recovers a dispersion relation, where the damping is given by $2\nu k^2$ and the water wave frequency ω_0 satisfies the usual gravity-capillary wave dispersion relation $\omega_0^2 = g_0 k + \Gamma k^3/\rho$.

In Figure 2 we present an example of the neutral stability curves $g_z(k)$ for the parameters used by Besson, *et al.* [7], and for various values of the parameter χ . These curves were obtained from (6) using the same method that Besson, *et al.* [7] used to obtain the neutral curves for the full hydrodynamic problem. The bicritical point in this example occurs at $\chi = 63.11^\circ$, for $g_z = 3.13 g_0$ ($g_0 = 980.665 \text{ cm/s}^2$), $k_+ = 7.14 \text{ cm}^{-1}$ and $k_- = 9.35 \text{ cm}^{-1}$, where k_\pm are the values of k associated with FMs ± 1 . The locations of the minima can be roughly approximated by considering the simple water wave dispersion relation $\omega_0^2 = g_0 k + \Gamma k^3/\rho$, and assuming

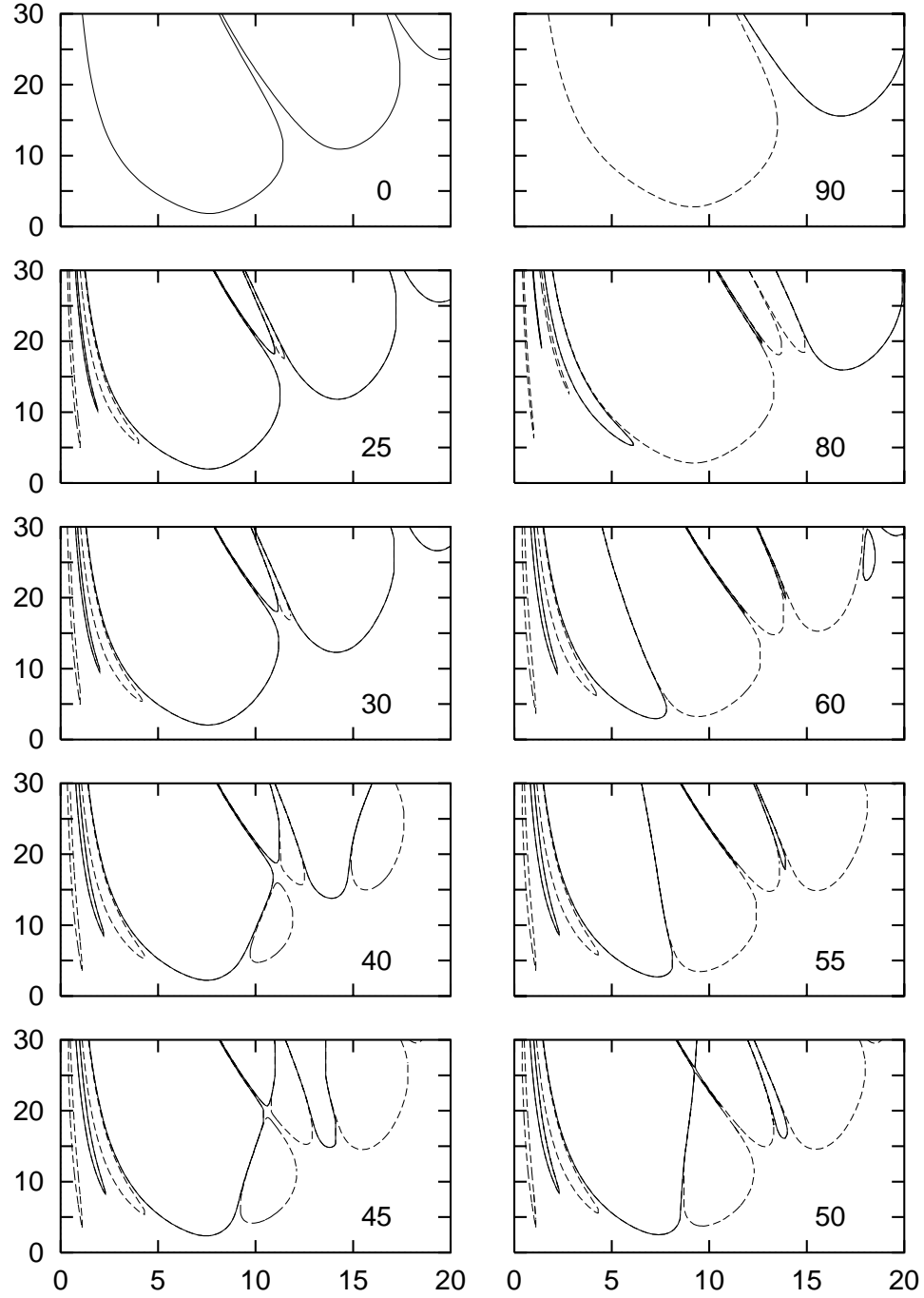


Figure 2: Neutral stability curves computed from (6). The vertical axis is g_z/g_0 and the horizontal axis is k ; the angle χ in (5) is indicated in the lower right corner of each plot. Floquet multipliers of $+1$ (-1) are indicated by solid (dashed) lines. The first instability encountered with increased forcing g_z is to harmonic waves if $\chi < \chi_c \approx 63^\circ$, and to subharmonic waves for $\chi > \chi_c$. The other parameters of the forcing function are $m = 4$, $n = 5$, $\phi = 0$ and $\omega/2\pi = 11$ Hz; the fluid parameters are $\Gamma = 20.6$ dyn/cm, $\nu = 0.209$ cm²/s and $\rho = 0.95$ g/cm³.

subharmonic response to the forcing frequencies at $m\omega$ and $n\omega$, *i.e.*, for $m = 4$ and $n = 5$:

$$\begin{aligned}\left(\frac{4\omega}{2}\right)^2 &\approx g_0 k_+ + \frac{\Gamma k_+^3}{\rho} \\ \left(\frac{5\omega}{2}\right)^2 &\approx g_0 k_- + \frac{\Gamma k_-^3}{\rho}\end{aligned}\tag{7}$$

For the example of Figure 2 this approximation yields $k_+ \approx 8.0$ and $k_- \approx 9.8$. We note that the neutral stability curves obtained from the simple linear problem (6) are qualitatively very similar to those obtained by Besson, *et al.* [7] from the full hydrodynamic problem, *cf.* our Figure 2 with Figure 2 in [7].

2.3 Normal form symmetries.

We now re-examine the role of resonant triad interactions for the mode interaction problem pertinent to the two-frequency Faraday experiment. In particular, we will investigate the additional effect of normal form symmetries on the pattern formation problem. We wish to contrast the situations where the forcing frequencies $m\omega$ and $n\omega$ in (5), $m < n$, have m even, n odd with m odd, n even. We are specifically interested in the case where the angle χ in (5) is close to the bicritical point χ_c .

We analyze the resonant triad interaction in terms of a stroboscopic map since we are interested in a periodically-forced system. We denote the surface height at time $t = pT$, p an integer, $T = 2\pi/\omega$, by $h_p(\mathbf{x})$. Let the resonant triad be

$$h_p = A_p e^{i\mathbf{k}_1 \cdot \mathbf{x}} + B_p e^{i\mathbf{k}_2 \cdot \mathbf{x}} + C_p e^{i(\mathbf{k}_1 + \mathbf{k}_2) \cdot \mathbf{x}} + c.c. + \dots,\tag{8}$$

where $|\mathbf{k}_1| = |\mathbf{k}_2| = k_m$ and $|\mathbf{k}_1 + \mathbf{k}_2| = k_n$, $0 < k_m < k_n < 2k_m$. Here the m, n subscripts indicate that the critical wavenumbers can be roughly associated with the $m\omega$ and $n\omega$ forcing, respectively, as in (7) above. The general form of the cubic-order amplitude equations, consistent with translation symmetry and reflection symmetry, is (*cf.* equation 3)

$$\begin{aligned}A_{p+1} &= \lambda A_p + \alpha B_p^* C_p + (a|A_p|^2 + b|B_p|^2 + c|C_p|^2)A_p \\ B_{p+1} &= \lambda B_p + \alpha A_p^* C_p + (a|B_p|^2 + b|A_p|^2 + c|C_p|^2)B_p \\ C_{p+1} &= \mu C_p + \beta A_p B_p + (d|A_p|^2 + d|B_p|^2 + e|C_p|^2)C_p.\end{aligned}\tag{9}$$

In the case that m is even and n is odd, the Floquet multipliers for the linearized problem are $\lambda = +1$ and $\mu = -1$ when $\chi = \chi_c$, whereas if m is odd and n is even, then $\lambda = -1$, $\mu = +1$.

It may be possible to further simplify the bifurcation problem (9) by a normal form transformation. In particular, there exists a near-identity nonlinear transformation such that all nonlinear terms in (9), which do not commute with the matrix L of the linearized problem, can be removed (see, for example, Crawford [26]). Here

$$L = \begin{pmatrix} \lambda & 0 & 0 \\ 0 & \lambda & 0 \\ 0 & 0 & \mu \end{pmatrix},\tag{10}$$

where $|\lambda| = |\mu| = 1$.

In the case that $\lambda = -1$, $\mu = +1$, *i.e.*, m odd and n even in the forcing (5), the bifurcation problem (9) is already in normal form since the normal form symmetry is equivalent to a translation by \mathbf{d} , where $\mathbf{k}_1 \cdot \mathbf{d} = \mathbf{k}_2 \cdot \mathbf{d} = \pi$. The presence of the quadratic terms in this normal form means that the resonant triad interactions will have a strong influence on the pattern formation problem, as described for the simple steady state bifurcation example in Section 2.1.

In contrast, in the case that $\lambda = +1$, $\mu = -1$, *i.e.*, m even and n odd, the normal form transformation allows the quadratic terms in the bifurcation problem to be removed. The normal form of the bifurcation problem, through cubic order, is

$$\begin{aligned} A_{p+1} &= A_p + (a|A_p|^2 + b|B_p|^2 + c|C_p|^2)A_p \\ B_{p+1} &= B_p + (a|B_p|^2 + b|A_p|^2 + c|C_p|^2)B_p \\ C_{p+1} &= -C_p + (d|A_p|^2 + d|B_p|^2 + e|C_p|^2)C_p . \end{aligned} \quad (11)$$

In this case, the bifurcation to harmonic waves is investigated in the invariant subspace $C = 0$, and there is no divergence of the cross-coupling term due to the resonant triad interaction. The usual contribution of the resonant triad interaction to the pattern formation problem is suppressed in this case. In the next section we test these ideas by performing explicit computations of bifurcation coefficients from the simplified hydrodynamic model, due to Zhang and Viñals [24], of the two-frequency Faraday experiment.

3 Two-frequency forcing of one-dimensional surface waves.

3.1 Resonant interactions in a one-dimensional problem.

It is possible to investigate the effects of strong spatial resonance on a pattern formation problem in one spatial dimension. This is done by considering the situation where the minima k_m and k_n of the neutral curve satisfy $k_m/k_n = 1/2$. In this case, the stroboscopic map associated with the critical modes $Z_p e^{ikx} + W_p e^{2ikx} + c.c.$ is, through cubic order,

$$\begin{aligned} Z_{p+1} &= \lambda Z_p + \alpha W_p Z_p^* + (a|Z_p|^2 + b|W_p|^2)Z_p \\ W_{p+1} &= \mu W_p + \beta Z_p^2 + (c|W_p|^2 + d|Z_p|^2)W_p . \end{aligned} \quad (12)$$

In form, this is identical to (9) restricted to the subspace $A = B = Z$, $C = W$.

If $\lambda = -1$ and $\mu = +1$, then (12) is already in normal form. The unfolding is

$$\begin{aligned} Z_{p+1} &= -(1 + \epsilon)Z_p + \alpha W_p Z_p^* + (a|Z_p|^2 + b|W_p|^2)Z_p \\ W_{p+1} &= (1 + \delta)W_p + \beta Z_p^2 + (c|W_p|^2 + d|Z_p|^2)W_p . \end{aligned} \quad (13)$$

Subharmonic waves bifurcate at $\epsilon = 0$. For $\delta \neq 0$, the center manifold is given by $W = -\beta Z^2/\delta + \dots$, and the branching equation is then given by

$$0 = -\epsilon + (a - \alpha\beta/\delta)|Z|^2 . \quad (14)$$

We see that the presence of the near critical spatially-resonant harmonic mode W forces the subharmonic wave to bifurcate with very small amplitude, since the cubic coefficient is large

when δ is small. This effect is the one-dimensional analogue of the cross-coupling term $g(\theta)$ diverging near a spatial resonance. This is the situation that can occur when m is odd and n is even ($n > m$) in (5), *e.g.* $m = 1, n = 2$.

If, on the other hand, $\lambda = +1, \mu = -1$, then the quadratic terms in (12) can be removed, and the usual effect of the spatial resonance on the pattern formation problem is suppressed. Specifically, the (unfolded) normal form of the bifurcation problem is

$$\begin{aligned} Z_{p+1} &= (1 + \epsilon)Z_p + (a|Z_p|^2 + b|W_p|^2)Z_p \\ W_{p+1} &= -(1 + \delta)W_p + (c|W_p|^2 + d|Z_p|^2)W_p . \end{aligned} \quad (15)$$

Harmonic waves, which bifurcate from the trivial solution at $\epsilon = 0$, are investigated in the invariant subspace $W = 0$; they satisfy the branching equation

$$0 = \epsilon + a|Z|^2 . \quad (16)$$

Subharmonic waves bifurcate from the trivial solution at $\delta = 0$ and can be investigated in the invariant subspace $Z = 0$; they satisfy the branching equation

$$0 = -\delta + c|W|^2 . \quad (17)$$

Neither of these branches is affected by the spatial resonance. This is the situation we expect when m is even and n is odd in (5), *e.g.* $m = 2, n = 3$.

In Figure 3, we plot the bicritical point χ_c as a function of ω for both $(m, n) = (2, 3)$ and $(m, n) = (1, 2)$. These curves apply to the linear equation (6), with $\Gamma = 20.6 \text{ dyn/cm}$, $\nu = 0.209 \text{ cm}^2/\text{s}$ and $\rho = 0.95 \text{ g/cm}^3$. In this figure we show also the ratio of wavenumbers k_n/k_m at the bicritical point. Note that in each case the spatial resonance $k_n/k_m = 2$ is achieved for a particular value of the forcing frequency $\omega = \omega^{res}$.

3.2 The Zhang-Viñals hydrodynamic model.

Zhang and Viñals [1] derive the following model for the surface deviation $h(\mathbf{x}, t)$ and surface velocity potential $\hat{\Phi}(\mathbf{x}, t)$, where $\mathbf{x} \in \mathbf{R}^2$:

$$\begin{aligned} (\partial_t - \hat{\gamma}\nabla^2)h - \hat{\mathcal{D}}\hat{\Phi} &= \tilde{\mathcal{F}}(h, \hat{\Phi}) \\ (\partial_t - \hat{\gamma}\nabla^2)\hat{\Phi} - \hat{\mathcal{A}}h &= \tilde{\mathcal{G}}(h, \hat{\Phi}) . \end{aligned} \quad (18)$$

Here the linear operator $\hat{\mathcal{A}}$ is

$$\hat{\mathcal{A}} \equiv \hat{\Gamma}_0 \nabla^2 - \hat{G}_0 - 4\hat{f}[\sin(2t) + \kappa \sin(2pt + \phi)] , \quad (19)$$

where $p = n/m$. The linear, nonlocal operator $\hat{\mathcal{D}}$ multiplies each Fourier component of the field by its wavenumber modulus. $\tilde{\mathcal{F}}$ and $\tilde{\mathcal{G}}$ are nonlinear operators to be defined shortly, together with the parameters $\hat{\gamma}, \hat{\Gamma}_0, \hat{G}_0, \hat{f}$ and κ .

In deriving the above, Zhang and Viñals assumed that the experimental forcing takes the form $g_z r(\sin(2m\omega_0 t) + \kappa \sin(2n\omega_0 t + \phi))$, where $\kappa \equiv (1 - r)/r$; they have scaled time by the frequency $m\omega_0$. Here we choose a slightly different scaling of time; we assume that the

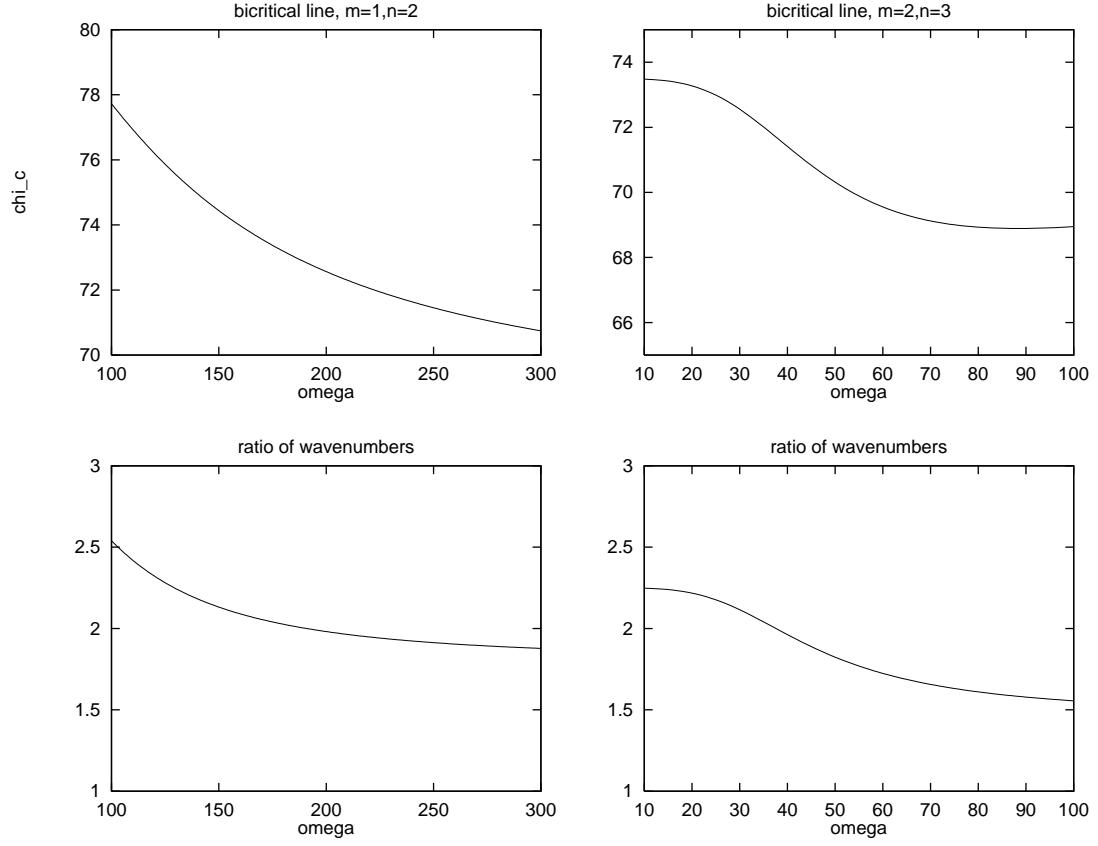


Figure 3: Bicritical point χ_c plotted as a function of the frequency ω in (5), where $\phi = 0$ and $\Gamma = 20.6 \text{ dyn/cm}$, $\nu = 0.209 \text{ cm}^2/\text{s}$ and $\rho = 0.95 \text{ g/cm}^3$ in (6). Plotted below each bicritical line is the ratio of critical wavenumbers k_n/k_m for $\chi = \chi_c(\omega)$. On the left $m = 1, n = 2$, and on the right $m = 2, n = 3$.

parametric forcing takes the (dimensionless) form $f[\cos(\chi)\cos(m\tau) + \sin(\chi)\cos(n\tau + \phi)]$. We let $t = m\tau/2$ and $\hat{\Phi} = \frac{2}{m}\Phi$ in (18) to obtain

$$\begin{aligned}(\partial_\tau - \gamma\nabla^2)h - \hat{\mathcal{D}}\Phi &= \mathcal{F}(h, \Phi) \\ (\partial_\tau - \gamma\nabla^2)\Phi - \mathcal{A}h &= \mathcal{G}(h, \Phi),\end{aligned}\tag{20}$$

where

$$\gamma \equiv \frac{2\nu k_0^2}{\omega}.\tag{21}$$

The wavenumber k_0 satisfies the equation

$$g_0 k_0 + \frac{\Gamma k_0^3}{\rho} = \frac{m^2 \omega^2}{4},\tag{22}$$

where $\omega = 2\omega_0$ is the dimensioned forcing frequency. The linear operator \mathcal{A} is now

$$\mathcal{A} \equiv \Gamma_0 \nabla^2 - G_0 - f(\cos(\chi)\cos(m\tau) + \sin(\chi)\cos(n\tau + \phi)),\tag{23}$$

where

$$\Gamma_0 \equiv \frac{\Gamma k_0^3}{\rho \omega^2}, \quad G_0 \equiv \frac{g k_0}{\omega^2}, \quad f \equiv \frac{g_z k_0}{\omega^2}.\tag{24}$$

The nonlinear operators are

$$\begin{aligned}\mathcal{F}(h, \Phi) &\equiv -\nabla \cdot (h\nabla\Phi) + \frac{1}{2}\nabla^2(h^2\hat{\mathcal{D}}\Phi) - \hat{\mathcal{D}}(h\hat{\mathcal{D}}\Phi) + \hat{\mathcal{D}}[h\hat{\mathcal{D}}(h\hat{\mathcal{D}}\Phi) + \frac{1}{2}h^2\nabla^2\Phi] \\ \mathcal{G}(h, \Phi) &\equiv \frac{1}{2}(\hat{\mathcal{D}}\Phi)^2 - \frac{1}{2}(\nabla\Phi)^2 - (\hat{\mathcal{D}}\Phi)[h\nabla^2\Phi + \hat{\mathcal{D}}(h\hat{\mathcal{D}}\Phi)] - \frac{1}{2}\Gamma_0\nabla \cdot (\nabla h(\nabla h)^2).\end{aligned}\tag{25}$$

Finally, we put the governing equations in a convenient form for the perturbation analysis that follows. In order to recover the linearized equation (6) for h , we apply the operator $(\partial_\tau - \gamma\nabla^2)$ to the first of equations (20), and then use the second equation to express $(\partial_\tau - \gamma\nabla^2)\Phi$ as $\mathcal{A}h + \mathcal{G}(h, \Phi)$. We supplement this equation with the first of equations (20), re-written as an equation for the field Φ , to obtain the full system of equations:

$$\begin{aligned}\mathcal{L}h &= (\partial_\tau - \gamma\nabla^2)\mathcal{F}(h, \Phi) + \hat{\mathcal{D}}\mathcal{G}(h, \Phi) \\ \hat{\mathcal{D}}\Phi &= (\partial_\tau - \gamma\nabla^2)h - \mathcal{F}(h, \Phi).\end{aligned}\tag{26}$$

Here the linear operator is

$$\mathcal{L} \equiv \partial_{\tau\tau} - 2\gamma\nabla^2\partial_\tau + (\gamma^2\nabla^4 - \hat{\mathcal{D}}\mathcal{A}),\tag{27}$$

where the operator \mathcal{A} is given by (23).

3.3 Weakly nonlinear analysis: derivation of the bifurcation problem.

We restrict our analysis to spatially one-dimensional solutions of the variable $x \in \mathbf{R}$, and use a two-timing perturbation method to determine weakly nonlinear solutions of the system (26) in

the vicinity of the bifurcation to (sub)harmonic waves, *i.e.* near a primary instability associated with a Floquet multiplier +1 (−1). To do this we introduce a small parameter ϵ , such that

$$\begin{aligned} h(x, \tau) &= \epsilon h_1(x, \tau, T) + \epsilon^2 h_2(x, \tau, T) + \epsilon^3 h_3(x, \tau, T) + \dots \\ \Phi(x, \tau) &= \epsilon \Phi_1(x, \tau, T) + \epsilon^2 \Phi_2(x, \tau, T) + \epsilon^3 \Phi_3(x, \tau, T) + \dots, \end{aligned} \quad (28)$$

where

$$T = \epsilon^2 \tau, \quad f = f_0 + \epsilon^2 f_2. \quad (29)$$

Here f_0 is the value of the forcing at the bifurcation point. We seek spatially-periodic solutions in the following separable Floquet-Fourier form:

$$\begin{aligned} h_1 &= z_1(T) p_1(\tau) e^{ik_c x} + c.c. & h_2 &= z_1^2(T) p_2(\tau) e^{i2k_c x} + c.c. \\ \Phi_1 &= z_1(T) q_1(\tau) e^{ik_c x} + c.c. & \Phi_2 &= z_1^2(T) q_2(\tau) e^{i2k_c x} + c.c. \end{aligned} \quad (30)$$

Here p_l, q_l ($l = 1, 2$) are 2π -periodic functions of the fast time τ in the case of harmonic waves (FM=+1); in the case of subharmonic waves they are 4π -periodic in τ . The wavenumber k_c is associated with the first unstable mode.

At leading order in ϵ , we obtain

$$\begin{aligned} \mathcal{L}_0 h_1 &= 0 \\ \widehat{\mathcal{D}} \Phi_1 &= (\partial_\tau - \gamma \partial_{xx}) h_1 \end{aligned} \quad (31)$$

Here the linear operator \mathcal{L}_0 is \mathcal{L} with $f = f_0$, where \mathcal{L} is defined by (27). The equation $\mathcal{L}_0 h_1 = 0$ determines the bifurcation point f_0 by the solvability condition that it have a periodic solution; it is the equation we solved in Section 2.2 to determine the neutral stability curves. This equation also determines the critical wavenumber k_c by the requirement that f_0 be the smallest value of f that admits a periodic solution. Given f_0 and k_c , we determine the solution of $\mathcal{L}_0 h_1 = 0$ involving the periodic function $p_1(\tau)$, which we may assume is real. We express p_1 in terms of its (truncated) Fourier series

$$p_1(\tau) = \sum_{j=0}^N a_j e^{i(j+\mu)\tau} + c.c., \quad (32)$$

where N is chosen large enough so that the solution is well converged. Here $\mu = 0$ for the case of harmonic waves and $\mu = 1/2$ for subharmonic waves. We readily solve the second of equations (31) for Φ_1 , yielding

$$q_1(\tau) = \frac{1}{k_c} (\partial_\tau + \gamma k_c^2) p_1. \quad (33)$$

At order ϵ^2 , we obtain

$$\begin{aligned} \mathcal{L}_0 h_2 &= -(\partial_\tau - \gamma \partial_{xx}) [\partial_x (h_1 \partial_x \Phi_1) + \widehat{\mathcal{D}}(h_1 \widehat{\mathcal{D}} \Phi_1)] + \frac{1}{2} \widehat{\mathcal{D}} [(\widehat{\mathcal{D}} \Phi_1)^2 - (\partial_x \Phi_1)^2] \\ &= 2k_c^3 z_1^2 q_1^2 e^{2ik_c x} + c.c., \end{aligned} \quad (34)$$

where q_1^2 is a real 2π -periodic function. We determine a solution h_2 involving the real periodic function $p_2(\tau)$, given by its (truncated) Fourier series representation

$$p_2 = \sum_{j=0}^N b_j e^{ij\tau} + c.c. \quad (35)$$

We also find, at this order, that Φ_2 satisfies

$$\widehat{\mathcal{D}}\Phi_2 = (\partial_\tau - \gamma\partial_{xx})h_2 \quad (36)$$

since $\partial_x(h_1\partial_x\Phi_1) + \widehat{\mathcal{D}}(h_1\widehat{\mathcal{D}}\Phi_1) = 0$; thus

$$q_2(\tau) = \frac{1}{2k_c}(\partial_\tau + 4\gamma k_c^2)p_2. \quad (37)$$

Finally, we consider the equation at order ϵ^3 :

$$\begin{aligned} \mathcal{L}_0 h_3 = & -2\partial_\tau\partial_T h_1 + 2\gamma\partial_{xx}\partial_T h_1 - f_2[\cos(\chi)\cos(m\tau) + \sin(\chi)\cos(n\tau + \phi)]\widehat{\mathcal{D}}h_1 \\ & + (\partial_\tau - \gamma\partial_{xx})\left[-\partial_x(h_1\partial_x\Phi_2 + h_2\partial_x\Phi_1) - \widehat{\mathcal{D}}(h_1\widehat{\mathcal{D}}\Phi_2 + h_2\widehat{\mathcal{D}}\Phi_1)\right] \\ & + \frac{1}{2}\partial_{xx}(h_1^2\widehat{\mathcal{D}}\Phi_1) + \widehat{\mathcal{D}}[h_1\widehat{\mathcal{D}}(h_1\widehat{\mathcal{D}}\Phi_1) + \frac{1}{2}h_1^2\partial_{xx}\Phi_1] + \widehat{\mathcal{D}}[(\widehat{\mathcal{D}}\Phi_1)(\widehat{\mathcal{D}}\Phi_2) \\ & - (\partial_x\Phi_1)(\partial_x\Phi_2) - \widehat{\mathcal{D}}\Phi_1[h_1\partial_{xx}\Phi_1 + \widehat{\mathcal{D}}(h_1\widehat{\mathcal{D}}\Phi_1)] - \frac{\Gamma_0}{2}\partial_x(\partial_x h_1)^3]. \end{aligned} \quad (38)$$

In order to ensure that a 2π -periodic solution exists, we must apply a solvability condition to this equation, written compactly as $\mathcal{L}_0 h_3 = H(x, \tau, T)$. Specifically, we require

$$\langle \widetilde{h}_1, \mathcal{L}_0 h_3 \rangle = \langle \widetilde{h}_1, H(x, \tau, T) \rangle = 0, \quad (39)$$

where the inner product is

$$\langle f, g \rangle \equiv \frac{k_c}{8\pi^2} \int_0^{4\pi} d\tau \int_0^{2\pi/k_c} f^*(x, \tau) g(x, \tau) dx; \quad (40)$$

$\widetilde{h}_1 \equiv \widetilde{p}_1(\tau)e^{ik_c x}$ is a periodic solution to the adjoint linear problem $\mathcal{L}_0^\dagger \widetilde{h}_1 = 0$. Here

$$\mathcal{L}_0^\dagger \equiv (\partial_\tau + \gamma\partial_{xx})^2 - \widehat{\mathcal{D}}\mathcal{A}, \quad (41)$$

where $f = f_0$ in \mathcal{A} .

The solvability condition leads to the amplitude equation

$$\delta \frac{dz_1}{dT} = \alpha f_2 z_1 + (A + B)|z_1|^2 z_1, \quad (42)$$

where

$$\delta = \frac{1}{2\pi} \int_0^{4\pi} (p_1' + i\mu p_1 + \gamma k_c^2 p_1) \widetilde{p}_1 d\tau$$

$$\begin{aligned}
\alpha &= \frac{-k_c}{4\pi} \int_0^{4\pi} [\cos(\chi) \cos(m\tau) + \sin(\chi) \cos(n\tau + \phi)] p_1 \tilde{p}_1 d\tau \\
A &= -\frac{k_c^2}{2\pi} \int_0^{4\pi} ((q_1 p_2)' + i\mu q_1 p_2 + \gamma k_c^2 q_1 p_2) \tilde{p}_1 d\tau \\
B &= \frac{k_c^3}{4\pi} \int_0^{4\pi} (-(p_1^2 q_1)' - i\mu p_1^2 q_1 - \gamma k_c^2 p_1^2 q_1 + k_c q_1^2 p_1 + \frac{3}{2} k_c^2 \Gamma_0 |p_1|^2 p_1) \tilde{p}_1 d\tau.
\end{aligned} \tag{43}$$

In the above, differentiation with respect to τ is denoted by a prime. We also took the periodic solution \tilde{p}_1 to be real.

In the above derivation of the bifurcation problem (42), we have separated the two contributions A and B to the cubic coefficient $A + B$. The contribution A comes from the quadratic nonlinear terms in the original hydrodynamic model; it depends on the spatially resonant modes $e^{i2k_c x}$ as is evident from the p_2 terms in the integral expression for A given in (43). The contribution B comes from cubic nonlinearities and therefore depends only on the mode $e^{ik_c x}$. We calculate all of the coefficients δ, α, A and B numerically as follows.

At leading order in ϵ , equation (31) for h_1 reduces to the linear problem (6). The solution for h_1 is found by representing $p_1(\tau)$ as the truncated Fourier series given in equation (32). As discussed in [7], the problem then reduces to a generalised eigenvalue problem of the form

$$\mathbf{A}\mathbf{x} = g_z \mathbf{B}\mathbf{x}, \tag{44}$$

where \mathbf{x} is a vector of the Fourier coefficients a_j in (32). The EISPACK routine `rgg` is used to find the eigenvalues and corresponding eigenvectors, the eigenvalues giving the linear stability curves shown in Figure 2. The eigenvalue corresponding to the minimum of the resonance tongue under consideration is then determined, with the corresponding eigenvector then giving the coefficients a_j for the spectral representation of $p_1(\tau)$, from which $q_1(\tau)$ can be calculated. The adjoint linear problem for \tilde{p}_1 is solved in a similar way to that for p_1 .

Once a spectral representation for q_1 is found, q_1^2 is calculated using a pseudospectral approach. This then enables the order ϵ^2 problem for h_2 , equation (34), to be written as a nonhomogeneous linear problem for p_2 . This can be solved using the EISPACK routine `rg`. Finally, the coefficients δ, α, A and B in the amplitude equation (42) are computed by calculating the various products of p_1, p_2 and q_1 using a pseudospectral method and then calculating the inner products.

Typically 20 Fourier modes sufficed to represent p_1, p_2 and q_1 , and 257 collocation points were adequate in the pseudospectral calculation of the nonlinear terms. Checks were done, with twice as many modes and collocation points, to ensure that the results were well converged.

In the next section we present plots of the ratio A/B of the two contributions to the cubic Landau coefficient for the case of bifurcation to waves excited with forcing frequency ratio $2/3$, and for the case of bifurcation to waves excited with forcing frequency ratio $1/2$.

4 Results.

We have calculated the coefficients δ, α, A and B in the amplitude equation (42) for four cases. These correspond to the two lowest resonance tongues in the two cases $m = 1, n = 2$ and $m = 2, n = 3$: whether harmonic or subharmonic waves bifurcate at a smaller value of the

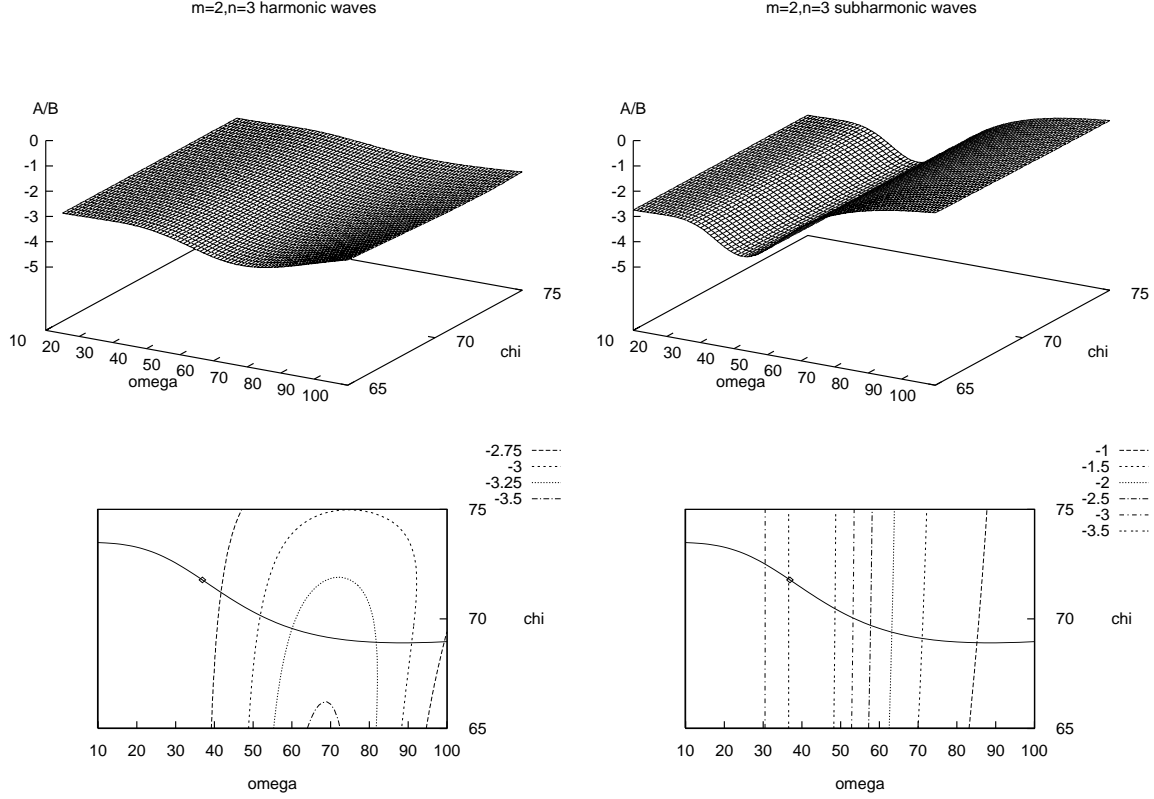


Figure 4: Plots of A/B as a function of χ and ω , for $m = 2$, $n = 3$ and $\phi = 0$ in (5). Computations are done at the bifurcation point to (sub)harmonic waves on the left (right). The fluid parameters are $\Gamma = 20.6 \text{ dyn/cm}$, $\nu = 0.209 \text{ cm}^2/\text{s}$ and $\rho = 0.95 \text{ g/cm}^3$. We give both surface plots (top) and the corresponding contour plots (below). In the contour plots we reproduce, from Figure 3, the bicritical line in the ω, χ -plane. The square on this curve gives the value of ω where the $1/2$ spatial resonance occurs.

driving amplitude depends on whether ω and χ take values which are above or below the bicritical lines given in Figure 3. The other parameters used are the same as those listed in the caption to Figure 3.

Figure 4 shows the ratio A/B of the two contributions to the cubic Landau coefficient for the excitation frequency ratio $2/3$ for the two tongues which bifurcate at lowest amplitudes of the parametric excitation, g_z . In each case the upper graphs show the surface representing A/B as a function of ω and χ . The lower graphs show the corresponding contour plots. Superimposed on the contour plot is the bicritical line from Figure 3 above: the square mark on this graph indicates the point on the bicritical line at which the ratio between the wavenumbers for the two minima is 2. Note that in this case, where the excitation frequency ratio is $2/3$, the bifurcation to the harmonic waves occurs at lower amplitudes of the parametric excitation g_z for values of ω and χ below the bicritical line, while the bifurcation to subharmonic waves occurs first for values of ω and χ above the bicritical line. The most striking feature of the plots associated with the harmonic waves in Figure 4 is the insensitivity of the quantity A/B to the point on the bicritical line at which the ratio between the wavenumbers is 2. Spatial resonance is also not important for the subharmonic waves since the subharmonic tongue occurs at the higher

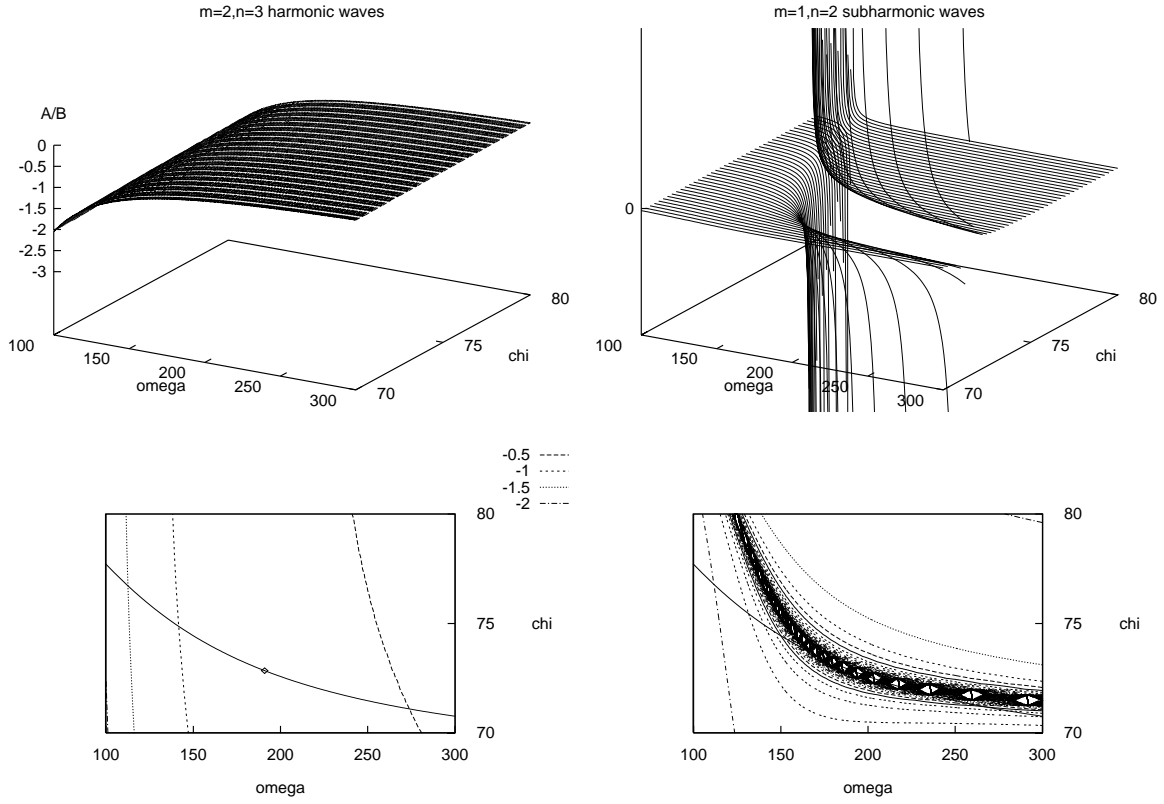


Figure 5: Plots of A/B similar to those in Figure 4, but computed for $m = 1$ and $n = 2$. The divergence of A/B for subharmonic waves is discussed in the text. This divergence occurs on a curve that is tangent to the bicritical line at the point $\omega^{res} = 191 \text{ s}^{-1}$, $\chi_c = 72.83^\circ$; this is the point where there is a $1/2$ spatial resonance on the bicritical line.

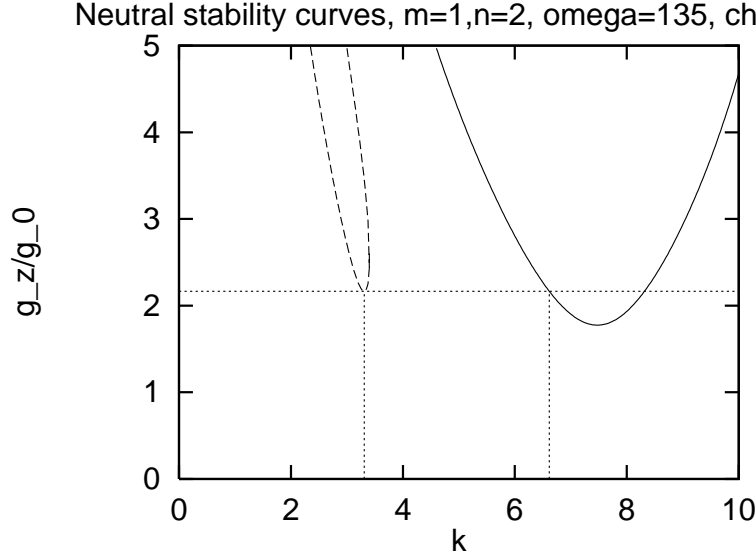


Figure 6: Neutral stability curves for $\omega = 135 \text{ s}^{-1}$, $\chi = 77.8^\circ$. The harmonic (subharmonic) tongue is indicated by a solid (dashed) line. The minimum of the subharmonic tongue occurs at $k_m = 3.308 \text{ cm}^{-1}$, when $g_z = 2.1658 g_0$. Also marked is the point where $2k_m$ intersects the harmonic tongue. Note that this intersection occurs at the critical value of g_z , where bifurcation to subharmonic waves occurs.

wavenumber in this case of even/odd excitation frequencies. This is in marked contrast to the case of odd/even excitation, as demonstrated by the graphs shown in Figure 5, which were computed for an excitation frequency ratio $1/2$. This time, it is the subharmonic instability which occurs first for values of ω and χ below the bicritical line and the harmonic instability which sets in first for values of ω and χ above the bicritical line. As for the previous graph, A/B for the harmonic waves is unaffected by the ratio between the wavenumbers and the parameter proximity to the bicritical line. However, in the case of subharmonic waves there is a singularity occurring on the bicritical line at the point of spatial resonance. This is consistent with the discussion in Section 3.1 above, showing how critical the nature of the instability is in determining whether or not spatial resonance is important to the pattern formation process near the bicritical line.

Note that in Figure 5 there is in fact a line of singularities tangent to the bicritical line at the point on the bicritical line where the ratio between the wavenumbers is $1/2$. This line of singularities can also be understood through spatial resonance. Recall that above the bicritical line the subharmonic instability occurs at a higher value of the excitation amplitude than the harmonic instability, as shown in Figure 6 for the values $\omega = 135 \text{ s}^{-1}$, $\chi = 77.8^\circ$. These values were chosen as representative of a point on the line of singularities shown in Figure 5.

In this case the minimum of the subharmonic tongue occurs at an excitation amplitude of $g_z = 2.1658 g_0$ and at a wavenumber of $k_m = 3.308 \text{ cm}^{-1}$. However, at this excitation amplitude there is a bifurcation to harmonic waves occurring at the wavenumber of $6.616 \text{ cm}^{-1} = 2k_m$, and therefore spatial resonance will occur. Similarly, for values of ω and χ to the right of the singularity which occurs on the bicritical line, spatial resonance can occur between the minimum of the subharmonic curve and the right side of the harmonic tongue. Note that, in practice, it is only close to the bicritical line that one would expect to observe the effect of the spatial resonance on the subharmonic waves, as in all other cases bifurcation to harmonic waves occurs at significantly lower amplitudes of the excitation. We also note that for parameters *on* the bicritical line the center manifold reduction described in Section 3.1 can break down.

5 Conclusions.

In this paper we have investigated how normal form symmetries affect the role of resonant triads in the pattern formation problem for surface waves parametrically excited by two-frequency forcing. We focused on the behavior of the system near the bicritical point in parameter space, where modes of wavenumber k_m and k_n lose stability simultaneously with one mode associated with a Floquet multiplier of $+1$ and the other associated with a Floquet multiplier of -1 . Our analysis shows that when the Floquet multiplier $+1$ is associated with the smaller wavenumber, then quadratic terms may be removed from the relevant amplitude equations. In this case, the contribution of resonant triads to the bifurcation problem is not affected by proximity to the bicritical point. In contrast, when the Floquet multiplier -1 is associated with the smaller wavenumber, then the quadratic terms cannot be removed by a normal form transformation. Hence, in this instance, resonant triads influence greatly the bifurcation problem near the bicritical point. The former situation applies when the forcing frequency ratio is $m/n < 1$, with m even and n odd, while the latter situation occurs when m is odd and n is even. Thus we expect normal form symmetries are important to understanding the experimentally observed quasipatterns and superlattice patterns [3, 5], which employ even/odd forcing. Such effects are necessarily neglected in theoretical models, such as the model of Lifshitz and Petrich [8], in which quasipatterns form through a steady state bifurcation.

This paper demonstrates the influence of the normal form symmetries on the bifurcation problem by considering the example of one-dimensional waves, parametrically excited by two-frequency forcing. In this one-dimensional problem a spatial resonance, involving Fourier modes of wavenumber k_m and $2k_m$, takes the place of a resonant triad. Specifically, we focused on the situation where the bicritical point involves modes k_m and $k_n = 2k_m$. We considered instability to harmonic waves and subharmonic waves when the two-frequency forcing was in ratio $m/n = 1/2$ and $m/n = 2/3$. Rather than perform the weakly nonlinear analysis on the full hydrodynamic equations, we used the simpler Zhang and Viñals model [1] that applies to a deep layer of a nearly inviscid fluid. Consistent with our general bifurcation theoretic analysis, we found that only in the case of subharmonic waves, parametrically excited by $m/n = 1/2$ -forcing, did the presence of the bicritical point lead to a diverging Landau coefficient in the bifurcation problem. In the other cases, the Landau coefficient was completely insensitive to any parameter proximity to the bicritical point or to the spatial resonance.

Our work suggests that the spatially resonant triads, important to a broad class of pattern

formation problems, do not play an important role in pattern formation of parametrically-excited surface waves near the bicritical point in the case of *even/odd* forcing. However, since our analysis focused only on the case of a one-dimensional pattern formation problem, more analysis in the two-dimensional case is warranted. In the future we hope to carry out a more extensive analysis of the contribution of resonant triads to two-dimensional Faraday waves with *even/odd* forcing. For instance, it would be of interest to carry out such an analysis for the physical parameters of the recent Faraday experiments in which superlattice patterns were observed [5]. In these experiments the forcing frequencies were in ratio 6/7; the spatial Fourier transform of the harmonic wave patterns exhibited peaks, some of which could be associated with the two different frequency components of the forcing wave form [5].

Although the analysis presented in this paper was motivated by and applied to the problem of Faraday waves with two-frequency forcing, we expect many of the symmetry-based ideas to carry over to other parametrically-excited pattern forming systems. We have in mind, for example, the recent experiments on one-dimensional surface waves on ferrofluids, which are excited by a time-periodic magnetic field [27]. In this system, both harmonic and subharmonic response occur with single-frequency forcing.

Acknowledgements.

We have benefited from discussions with Laurette Tuckerman. The research of MS was supported by an NSF CAREER award DMS-9502266.

References

- [1] W. Zhang and J. Viñals. Pattern formation in weakly damped parametric surface waves driven by two frequency components. *J. Fluid Mech.* **341** 225–244 (1998).
- [2] W.S. Edwards and S. Fauve. Parametrically excited quasicrystalline surface waves. *Phys. Rev. E* **47** R788–R791 (1993).
- [3] W.S. Edwards and S. Fauve. Patterns and quasi-patterns in the Faraday experiment. *J. Fluid Mech.* **278** 123–148 (1994).
- [4] H.W. Müller. Periodic triangular patterns in the Faraday experiment. *Phys. Rev. Lett.* **71** 3287–3290 (1993).
- [5] A. Kudrolli, B. Pier and J.P. Gollub. Superlattice patterns in surface waves. *Physica D*, in press (1998).
- [6] J. Beyer and R. Friedrich. Faraday instability: linear analysis for viscous fluids. *Phys. Rev. E* **51** 1162–1168 (1995).
- [7] T. Besson, W.S. Edwards and L.S. Tuckerman. Two-frequency parametric excitation of surface waves. *Phys. Rev. E* **54** 507–513 (1996).
- [8] R. Lifshitz and D.M. Petrich. Theoretical model for Faraday waves with multiple-frequency forcing. *Phys. Rev. Lett.* **79** 1261–1265 (1997).

- [9] M. Silber and M.R.E. Proctor. Nonlinear competition between small and large hexagonal patterns. *Phys. Rev. Lett.* **81** 2450–2453 (1998).
- [10] M. Faraday. On the forms and states of fluids on vibrating elastic surfaces. *Phil. Trans. R. Soc. Lond.* **52** 319–340 (1831).
- [11] For a review, see J. Miles and D. Henderson. Parametrically forced surface waves. *Annu. Rev. Fluid Mech.* **22** 143–165 (1990).
- [12] B. Christiansen, P. Alstrøm and M.T. Levinsen. Ordered capillary-wave states: quasicrystals, hexagons, and radial waves. *Phys. Rev. Lett.* **68** 2157–2160 (1992).
- [13] B. Christiansen, P. Alstrøm and M.T. Levinsen. Dissipation and ordering in capillary waves at high aspect ratios. *J. Fluid Mech.* **291** 323–341 (1995).
- [14] D. Binks and W. van de Water. Nonlinear pattern formation of Faraday waves. *Phys. Rev. Lett.* **78** 4043–4046 (1997).
- [15] J. Bechhoefer, V. Ego, S. Manneville, and B. Johnson. An experimental study of the onset of parametrically pumped surface waves in viscous fluids. *J. Fluid Mech.* **288** 325–350 (1995).
- [16] A. Kudrolli and J.P. Gollub. Patterns and spatiotemporal chaos in parametrically forced surface waves: a systematic survey at large aspect ratio. *Physica D* **97** 133–154 (1996).
- [17] K. Kumar and L.S. Tuckerman. Parametric instability of the interface between two fluids. *J. Fluid Mech.* **279** 49–68 (1994).
- [18] K. Kumar. Linear theory of Faraday instability in viscous liquids. *Proc. R. Soc. Lond. A* **452** 1113–1126 (1996).
- [19] H.W. Müller, H. Wittmer, C. Wagner, J. Albers and K. Knorr. Analytic stability theory for Faraday waves and the observation of the harmonic surface response. *Phys. Rev. Lett.* **78** 2357–2360 (1997).
- [20] M. Golubitsky, J.W. Swift and E. Knobloch. Symmetries and pattern selection in Rayleigh–Bénard convection. *Physica D* **10** 249–276 (1984).
- [21] M.C. Cross and P.C. Hohenberg. Pattern formation outside of equilibrium. *Rev. Mod. Phys.* **65** 851–1112 (1993).
- [22] A.C. Newell and Y. Pomeau. Turbulent crystals in macroscopic systems. *J. Phys. A* **26** L429–L434 (1993).
- [23] P. Chen and J. Viñals. Pattern selection in Faraday waves. *Phys. Rev. Lett.* **79** 2670–2673 (1997).
- [24] W. Zhang and J. Viñals. Pattern formation in weakly damped parametric surface waves. *J. Fluid Mech.* **336** 301 (1998).

- [25] B. Dionne, M. Silber and A.C. Skeldon. Stability results for steady, spatially-periodic planforms. *Nonlinearity* **10** 321–353 (1997).
- [26] J.D. Crawford. Introduction to bifurcation theory. *Rev. Mod. Phys.* **63** 991–1037 (1991).
- [27] T. Mahr and I. Rehberg. Magnetic Faraday-instability. *Europhys. Lett.* **43** 23–28 (1998).